Prediction of Rough-Wall Skin Friction and Heat Transfer

George H. Christoph*
Science Applications, Inc., Wayne, Pennsylvania
and
Richard H. Pletcher†
Iowa State University, Ames, Iowa

A finite difference solution to the boundary-layer equations for flow over rough surfaces is presented. The boundary-layer equations are cast in a form to account for the blockage effects of roughness elements. The roughness effect is described by a sink term in the momentum equation and a source term in the static enthalpy equation. A two-layer algebraic mixing length model that accounts for low Reynolds numbers, surface roughness, and wall transpiration is developed. Good agreement is shown for several comparisons to rough-wall, flat-plate and sharp-cone data.

Nomenclature

A^+ = van Driest constant, = 26
$B(y)$ = function defined by Eq. (11)
c_D = form drag coefficient
c_f = skin friction coefficient, $=2\tau_w/(\rho_e u_e^2)$
$D(y)$ = roughness element diameter
D_a = viscous damping function
$f(y)$ = function defined by Eq. (11)
F = variable defined by Eq. (7)
h = static enthalpy
H = total enthalpy, $=h+u^2/2$
I = variable defined by Eq. (7)
k = thermal conductivity
K = roughness height
K_{es} = equivalent sand grain roughness height
K^+ = Ku^*/ν_w
ℓ = mixing length
L = roughness element spacing
L_r = arbitrary constant in Mangler transformation
M = Mach number
P = static pressure
Pr = Prandtl number
$\dot{q}$ = heat flux
r = radial distance from axis of symmetry
r_0 = body radius
Re_s = $u_e s/\nu_e$
Re_θ = $u_e\theta/\nu_e$
s = wetted length measured from stagnation point
St = Stanton number, $=\dot{q}_w/[\rho_e u_e(h_{aw}-h_w)]$
t = dimensionless parameter, $=r/r_0$
T = temperature
u = streamwise velocity
u^* = friction velocity, $=(\tau_w/\rho_w)^{1/2}$
u^+ = u/u^*
v = normal velocity
$\tilde{v}$ = normal velocity, $=(\rho v+\overline{\rho' v'})/\rho$
V = variable defined by Eq. (7)
v_w^+ = v_w/u^*
y = coordinate normal to s
y^+ = yu^*/ν_w
z = function defined by Eq. (25)
β = dimensionless parameter, $=(\xi/u_e)/(du_e/d\xi)$
δ = boundary-layer thickness
η = transformed normal coordinate defined by Eq. (6)
θ = momentum thickness
μ = viscosity
ν = kinematic viscosity
ξ = transformed streamwise coordinate defined by Eq. (6)
ρ = density
τ = shear stress

Subscripts

aw = adiabatic wall
e = edge
i = inner
o = outer
r = rough
s = smooth
t = turbulent
w = wall
FT = fully turbulent
∞ = freestream

Superscripts

$(\ )'$ = fluctuating quantities
$(\bar{\ })$ = time mean quantities

Introduction

SURFACE roughness can significantly affect turbulent skin friction and heat transfer in many applications. The NASA Space Shuttle Program studied roughness as it affects augmented heating. More recently, maneuvering vehicle control effectiveness has been shown to be dramatically influenced by roughness on the control surface and on the forebody ahead of the control panel.[1]

Most roughness analyses are based on Nikuradse's sand grain experiments and the "law of the wall" velocity profiles fit to these data. Several correlations have been proposed to relate real roughness heights, spacings, and geometries to an equivalent sand grain roughness height so that Nikuradse's data can be used. Examples of such correlations can be found in Bettermann,[2] Dirling,[3] and White and Grabow.[4] More recently, surface roughness calculations have been performed by differential methods. Cebeci and Chang[5] numerically solved the incompressible boundary-layer equations employing an algebraic eddy viscosity formulation modified for surface roughness. The modification was based on Rotta's model,[6] which displaces the normal coordinate of the rough-wall velocity profile. An expression for this displacement, and the resulting mixing length, is given by Cebeci and Chang as a function of an equivalent sand grain roughness height. Emphasizing compressible flows for a variety of edge and wall conditions, Hodge and Adams[7] numerically solved the boundary-layer equations and an integral form of the equation for kinetic energy of turbulence. Roughness effects

Presented as Paper 82-0031 at the AIAA 20th Aerospace Sciences Meeting, Orlando, Fla., Jan. 11-14, 1982; submitted Jan. 20, 1982; revision received July 6, 1982.

*Senior Staff Scientist. Member AIAA.
†Professor of Mechanical Engineering. Member AIAA.

were accounted for by a form drag term in the momentum equation and by modifications, based on the results of Healzer et al.,[8] for several of the nine empirical constants. It is the intent of this paper to present a numerical technique for calculating skin friction and heat transfer over surfaces with real roughness, using as little empiricism as possible.

Contriving an equivalent sand grain roughness height for real roughness heights, spacings, and geometries is not very satisfying. A physically more meaningful method that accounts for actual roughness effects is that employed by Finson and Clarke[9] and Lin and Bywater.[10] These techniques calculate the form drag contributions of individual elements. Roughness elements are assumed to occupy no physical space. The governing boundary-layer equations are cast in a form to account for the blockage effects of the roughness elements. Following Finson and Clarke, terms that act in the streamwise direction are multiplied by $[1-D(y)/L]$ where $D(y)$ is the element diameter at height y and L the average center-to-center spacing. Terms that act in a direction normal to the streamwise direction are multiplied by $[1-\pi D^2(y)/4L^2]$. The effect of roughness is described by a sink term in the momentum equation and by a source term in the static enthalpy equation.

When the above approach is adopted, one must examine carefully the turbulence model used. Existing rough-wall, mixing length models are expressed in terms of an equivalent sand grain roughness height and are validated for the boundary-layer equations without blockage effects or source and sink terms (e.g., Cebeci and Chang[5] or Healzer et al.[8]). Lin and Bywater modify their turbulent kinetic energy model equation to include blockage effects. Finson and Clarke[9] use a second-order closure approximation for their turbulence model, describing the effect of roughness by distributed source or sink terms in the appropriate equations. These latter two methods are still left with modeling constants whose roughness effects are uncertain. In the present study, it was decided to use a two-layer algebraic mixing length model, building to more complex models if necessary. A mixing length model is proposed that explicitly includes roughness height, frequency, and type by applying concepts from the analyses of Pletcher[11] and White and Christoph.[12]

Equations and Solution Procedures

Governing Equations

For an axisymmetric, steady, compressible turbulent flow, the standard boundary-layer equations are

Continuity

$$\frac{\partial}{\partial s}(\rho u r)+\frac{\partial}{\partial y}(\rho\tilde{v}r)=0 \tag{1}$$

Momentum

$$\rho u\frac{\partial u}{\partial s}+\rho\tilde{v}\frac{\partial u}{\partial y}=\rho_e u_e\frac{\mathrm{d}u_e}{\mathrm{d}s}+\frac{1}{r}\frac{\partial}{\partial y}\left[r\left(\mu\frac{\partial u}{\partial y}-\rho\overline{v'u'}\right)\right] \tag{2}$$

Energy

$$\rho u\frac{\partial H}{\partial s}+\rho\tilde{v}\frac{\partial H}{\partial y}=\frac{1}{r}\frac{\partial}{\partial y}\left(r\left\{\frac{\mu}{Pr}\frac{\partial H}{\partial y}-\rho\overline{v'h'}+u\left[\left(1-\frac{1}{Pr}\right)\mu\frac{\partial u}{\partial y}-\rho\overline{v'u'}\right]\right\}\right) \tag{3}$$

The coordinate s is measured along the surface from the stagnation point, and the coordinate y is perpendicular to s. The boundary conditions imposed are at $y=0$, $u(s,0)=0$, $v(s,0)=v_w(s)$, $H(s,0)=H_w(s)$, or $(\partial H/\partial y)_{y=0}$ specified, and as $y\to\infty$, $u(s,y)=u_e(s)$ and $H(s,y)=H_e(s)$. In the above, $\tilde{v}=(\rho v+\rho' v')/\rho$. The terms $-\rho\overline{v'u'}$ and $\rho\overline{v'h'}$ represent the apparent turbulent shear stress and heat flux, respectively, and must be modeled.

Equations (1-3) are now recast, in the manner proposed by Finson and Clarke,[9] to account for roughness. As discussed in the Introduction, terms that act in the streamwise direction are multiplied by $[1-D(y)/L]$, and terms that act normal to the streamwise direction are multiplied by $[1-\pi D^2(y)/(4L^2)]$. A form drag term

$$-\tfrac{1}{2}\rho u^2 c_D D(y)/L^2 \tag{4}$$

is added to the momentum equation, and a source term

$$\tfrac{1}{2}\rho u^3 c_D D(y)/L^2 \tag{5}$$

is added to the static enthalpy equation such that the total enthalpy is not altered.

Also, a combination of the Levy-Lees and Mangler transformations is used to remove the stagnation point singularity. Such a transformation permits very accurate solutions to be obtained near the stagnation point and results in a more gradual growth of the boundary-layer thickness in terms of the transformed normal coordinate. The transformed coordinates are defined by

$$\xi=\int_0^s\frac{r_0^2}{L_r^2}\,\mathrm{d}s,\qquad \eta=\left(\frac{u_e}{\rho_e\mu_e\xi}\right)^{1/2}\int_0^y\frac{r}{L_r}\rho\,\mathrm{d}y \tag{6}$$

where r is the radial distance from the axis of symmetry, r_0 the body radius, and L_r an arbitrary reference length. The dependent variables are nondimensionalized according to

$$F=\frac{u}{u_e},\quad I=\frac{H}{H_e},\quad V=\rho\tilde{v}\left(\frac{\xi}{u_e\rho_e\mu_e}\right)^{1/2}\frac{L_r r}{r_0^2}+\frac{\xi L_r^2 f(y)F}{r_0^2}\frac{\partial\eta}{\partial s} \tag{7}$$

Utilizing Eqs. (6) and (7) and the roughness modifications, the conservation equations become

Continuity

$$f(y)\frac{\partial}{\partial\xi}\left[(u_e\rho_e\mu_e\xi)^{1/2}F\right]+\frac{\partial}{\partial\eta}\left[\left(\frac{u_e\rho_e\mu_e}{\xi}\right)^{1/2}V\right]=0 \tag{8}$$

Momentum

$$\xi f(y)F\frac{\partial F}{\partial\xi}+V\frac{\partial F}{\partial\eta}=f(y)\beta(\rho_e/\rho-F^2)+\frac{1}{B(y)}\frac{\partial}{\partial\eta}\left(t^2\frac{\rho\tilde{\mu}B(y)}{\rho_e\mu_e}\frac{\partial F}{\partial\eta}\right)-\tfrac{1}{2}\frac{c_D D(y)\xi F^2}{r_0^2L^2B(y)} \tag{9}$$

Energy

$$\xi f(y)F\frac{\partial I}{\partial\xi}+V\frac{\partial I}{\partial\eta}=\frac{1}{B(y)}\frac{\partial}{\partial\eta}\left\{B(y)\left(\frac{\mu}{Pr}+\frac{\mu_t}{Pr_t}\right)\frac{\rho t^2}{\rho_e\mu_e}\frac{\partial I}{\partial\eta}+B(y)\frac{\rho u_e^2Ft^2}{H_e\rho_e\mu_e}\left[\mu\left(1-\frac{1}{Pr}\right)+\mu_t\left(1-\frac{1}{Pr_t}\right)\right]\frac{\partial F}{\partial\eta}\right\} \tag{10}$$

The functions $B(y)$ and $f(y)$ are defined by

$$B(y) = 1 - \pi D^2(y)/(4L^2)$$
$$f(y) = [1 - D(y)/L]/B(y) \tag{11}$$

and the parameters β and t are defined as

$$\beta = \frac{\xi}{u_e}\frac{du_e}{d\xi}, \qquad t = \frac{r}{r_0} \tag{12}$$

In the above, the Boussinesq assumption has been employed to evaluate the shear stress; that is, it has been assumed that

$$\tau = \mu\frac{\partial u}{\partial y} - \rho\overline{v'u'} = (\mu + \mu_t)\frac{\partial u}{\partial y} = \bar{\mu}\frac{\partial u}{\partial y} \tag{13}$$

It has been further assumed that the turbulent heat flux can likewise be represented through the Boussinesq assumption. Representing turbulent conductivity by

$$k_t = c_p\mu_t/Pr_t \tag{14}$$

where the turbulent Prandtl number was set equal to a constant value of 0.9, the turbulent heat flux can be evaluated as

$$-\rho\overline{v'h'} = \frac{\mu_t}{Pr_t}\frac{\partial h}{\partial y} = \frac{\mu_t}{Pr_t}\frac{\partial H}{\partial y} - \frac{\mu_t}{Pr_t}u\frac{\partial u}{\partial y} \tag{15}$$

Equations (13-15) were employed to eliminate the Reynolds stress and heat flux terms prior to transforming the equations. The boundary conditions for the new variables are given by

$$F(s,0) = 0, \qquad V(s,0) = \rho_w\tilde{v}_w\left(\frac{\xi}{u_e\rho_e\mu_e}\right)^{1/2}\frac{L_r}{r_0}$$
$$I(s,0) = I_w(s) \text{ or } \left.\frac{\partial I}{\partial\eta}\right|_{\eta=0} \text{ specified}$$

and as

$$\eta \to \infty, \qquad F = I = 1.0 \tag{16}$$

Turbulence Modeling

Prandtl's mixing length hypothesis is used to evaluate the apparent turbulent viscosity according to

$$\mu_t = \rho\ell^2\left|\frac{\partial u}{\partial y}\right| \tag{17}$$

The mixing length is evaluated as

$$\ell_i = 0.41D_a y \tag{18}$$

in the inner region and

$$\ell_o = 0.089\delta \tag{19}$$

in the outer region where D_a is a modified van Driest damping function and δ is the boundary-layer thickness. The damping function and the form of the mixing length [Eq. (18)] must be specified for such complicating effects as wall transpiration and surface roughness. For incompressible flow over an impermeable smooth wall, van Driest[13] recommended

$$D_a = 1 - \exp(-y^+/A^+) \tag{20}$$

where $A^+ = 26$. Pletcher[11] modified this form for transpired flows by setting

$$D_a = 1 - \exp(-z) \tag{21}$$

where

$$z = (y^+/26)(\tau/\tau_w)^{1/2}(\tau_{FT}/\tau_w)^{1/2} \tag{22}$$

and τ_{FT} is the shear stress near the beginning of the fully turbulent region. This form for z was proposed to account for shear stress variations near a wall. Utilizing the analysis of Ref. 11, which made use of Simpson's "law of the wall with blowing,"[14] τ_{FT} was expressed as

$$\tau_{FT}/\tau_w = 1 + 1.092v_w^{+2} + 2.09(1 + 11v_w^+)^{1/2} + 11v_w^+ \tag{23}$$

where

$$v_w^+ = \tilde{v}_w/(\tau_w/\rho_w)^{1/2} \tag{24}$$

If the shear stresses in Eq. (22) are rough-wall values, one would expect the smooth-wall constant, $A^+ = 26$, to change. Instead of trying to find a new empirical constant/function for rough walls, let us try multiplying the right-hand side of Eq. (22) by τ_{wr}/τ_{ws} where the subscripts r and s represent rough and smooth values, respectively. Then

$$z = \frac{y^+}{26}\left(\frac{\tau_r}{\tau_{wr}}\right)^{1/2}\left(\frac{\tau_{FTr}}{\tau_{wr}}\right)^{1/2}\left(\frac{\tau_{wr}}{\tau_{ws}}\right) \tag{25}$$

An expression for τ_{FTr} is obtained by neglecting the convective acceleration and by evaluating the momentum equation at the top of the roughness elements ($y = K$). Then

$$\tau_{FTr} = \tau_{ws} + \frac{1}{2}\int_0^K \frac{f(y)\rho u^2 c_D D(y)}{B(y)L^2}\,dy + K\frac{dP_e}{ds} \tag{26}$$

where the effect of wall transpiration is neglected since it is accounted for in Eq. (23). As the roughness height increases, the damping factor approaches 1, as expected.

It is also necessary to modify the mixing length formulation [Eq. (18)] for roughness effects. Healzer et al.[8] and Cebeci and Chang[5] suggest mixing length modifications for sand grain roughness. For the present study, a mixing length was derived based on the "law of the wall" analysis of White and Christoph.[12] For illustrative purposes, the derivation presented here considers incompressible flow and ignores wall transpiration and pressure gradient effects. First, approximate the turbulent shear using Prandtl's mixing length hypothesis according to Eqs. (17) and (18). Then, note that near the wall there is negligible convective acceleration, so that an expression for τ_w, such as Eq. (26), holds. Combining these results gives an expression for $\partial u^+/\partial y^+$. (This result can be found in Ref. 15 for arbitrary wall and edge conditions.) For fully turbulent flow with roughness, one has

$$\frac{\partial u^+}{\partial y^+} = \left[\frac{\tau_{ws}}{\tau_{wr}} + \frac{1}{2}\int_0^{K^+}\frac{\nu_w c_D f(y^+)u^{+2}D(y^+)}{u^* L^2 B(y^+)}\,dy^+\right]^{1/2}\Big/0.41y^+ \tag{27}$$

Note that for a smooth wall one obtains

$$\frac{\partial u^+}{\partial y^+} = \frac{1}{0.41y^+} \tag{28}$$

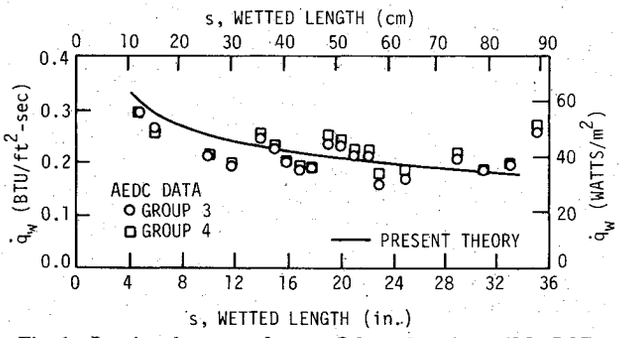

Fig. 1 Laminar heat transfer on a 7 deg sphere/cone ($M=5.95$).

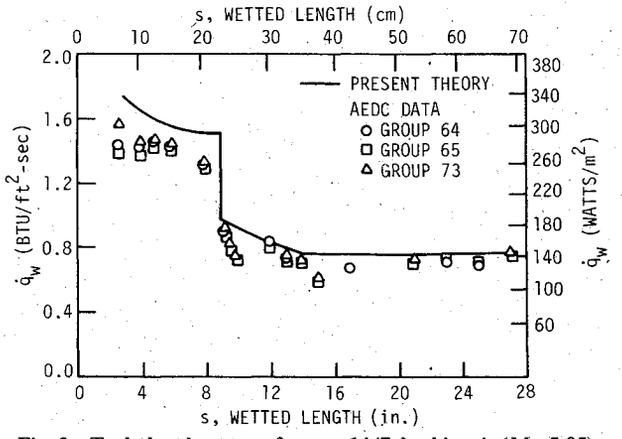

Fig. 2 Turbulent heat transfer on a 14/7 deg biconic ($M=5.95$).

ROUGHNESS ELEMENTS	DIMENSION	L (cm)	D (cm)	K (cm)	K_{es} (cm)
SPHERES	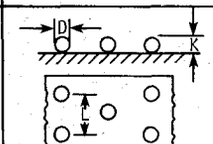	4	0.41	0.41	0.093
		2	0.41	0.41	0.344
		1	0.41	0.41	1.260
		0.6	0.41	0.41	1.560
		1	0.21	0.21	0.172
		0.5	0.21	0.21	0.759
SPHERICAL SEGMENTS	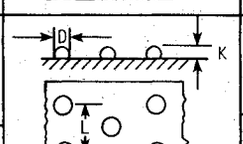	4	0.8	0.26	0.031
		3	0.8	0.26	0.049
		2	0.8	0.26	0.149
CONES		4	0.8	0.375	0.059
		3	0.8	0.375	0.164
		2	0.8	0.375	0.374

Fig. 3 Schlichting arrangement of roughness elements.[16]

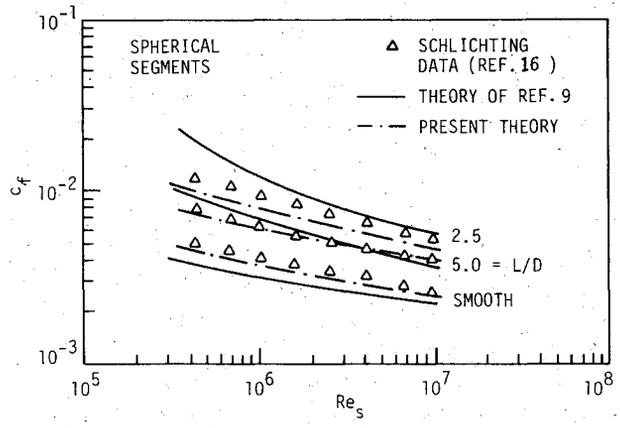

Fig. 4 Skin friction coefficients for Schlichting's roughness data.

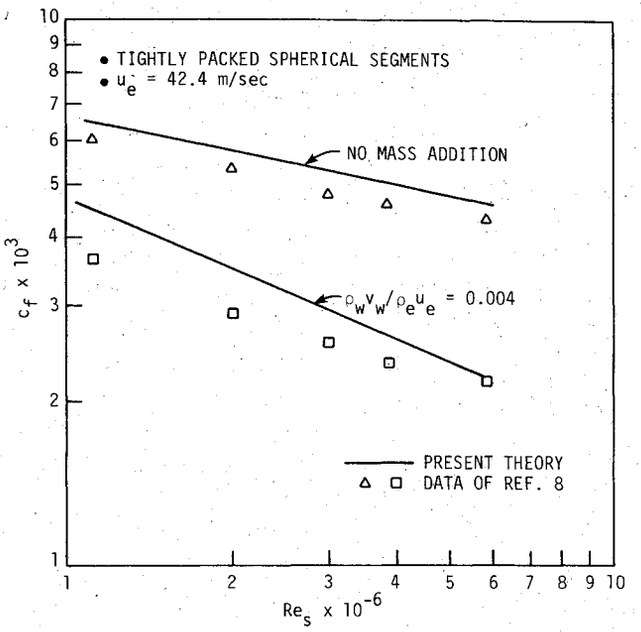

Fig. 5 Rough surface skin friction predictions vs data of Healzer et al.

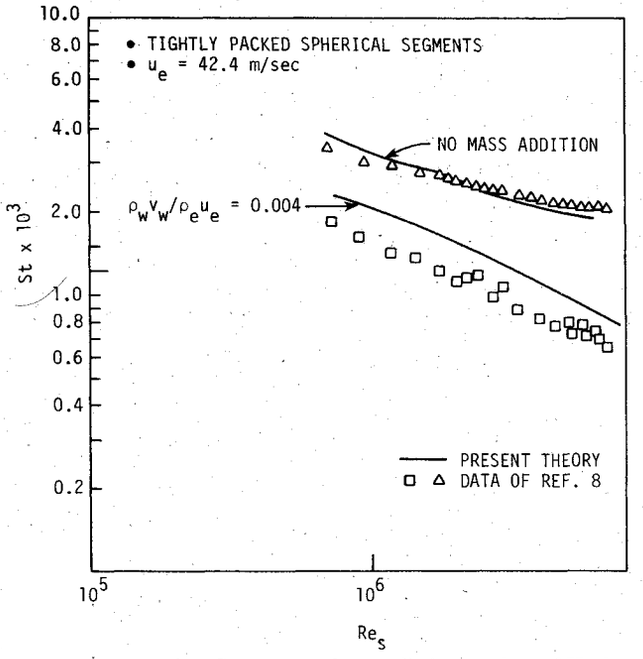

Fig. 6 Rough surface Stanton number predictions vs data of Healzer et al.

where $\ell=0.41y$. This suggests that for a rough surface

$$\ell=0.41y\Big/\left[\frac{\tau_{ws}}{\tau_{wr}}+\frac{1}{2}\int_0^{K^+}\frac{\nu_w c_D f(y^+)u^{+2}D(y^+)}{u^* L^2 B(y^+)}\,dy^+\right]^{1/2} \quad (29)$$

For the present study, the rough-wall mixing length was derived to include compressibility, mass addition, and pressure gradient effects. Finally, it should be remarked that the "law of the wall" profiles, outlined above and given in Ref. 15, were found to be in reasonable agreement with the roughness channel flow data of Schlichting.[16] This is a partial verification for the form of the damping function given in Eq. (25) and the mixing length modification just discussed.

The switch point from the inner [Eq. (18)] to the outer [Eq. (19)] model was made in accordance with the low

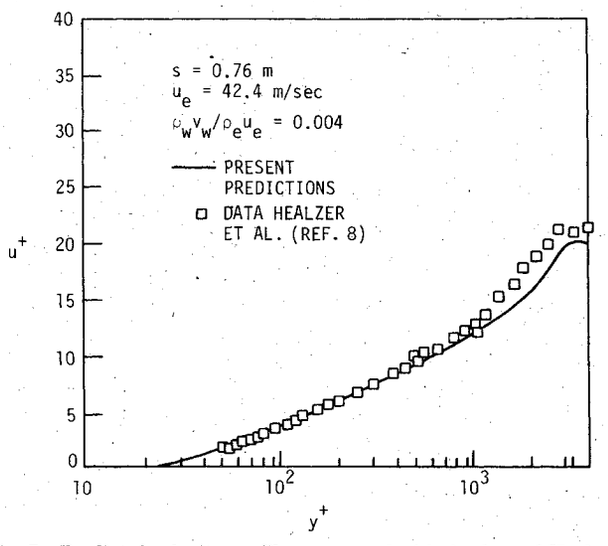

Fig. 7 Predicted velocity profiles compared with the data of Healzer et al., combined roughness (tightly packed spherical elements) and blowing.

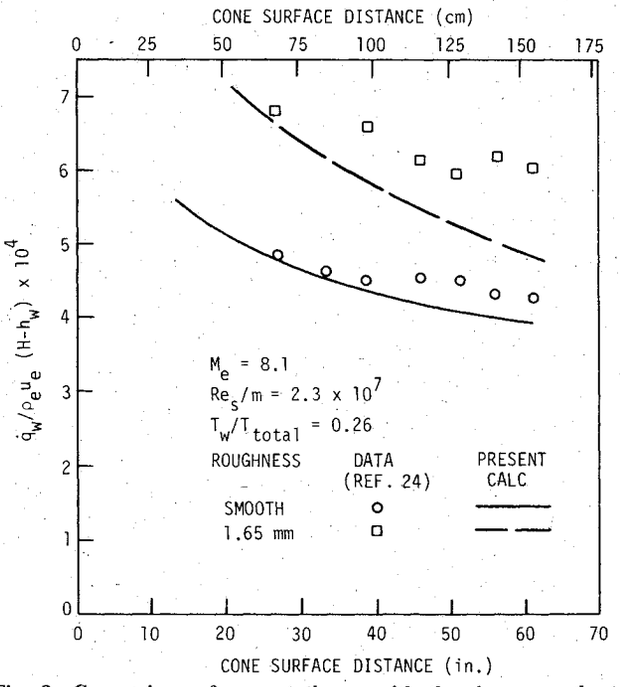

Fig. 8 Comparison of present theory with the sharp-cone heat-transfer data of Hill et al.

Reynolds number modification presented in Ref. 17. This provides that the switch be made at the point when ℓ_i first becomes equal to ℓ_o provided that $y^+ \geq 50$. If $y^+ < 50$ when $\ell_i = \ell_o$, then the switch point is delayed until y^+ becomes equal to 50 and ℓ_o becomes equal to ℓ_i at $y^+ = 50$. This prevents the suppression of the fully turbulent portion of the velocity profile that can occur at low values of Re_θ. This effect persists to higher and higher values of Re_θ as the Mach number increases.

Method of Solution

Equations (8-10) were solved numerically by a fully implicit finite difference procedure. Streamwise derivatives were approximated to second-order accuracy by using three-point difference representations. Second-order accuracy for the convective terms was maintained without iterations by the use of extrapolated values of the coefficients. Unequal grid spacing in the normal direction was implemented by a

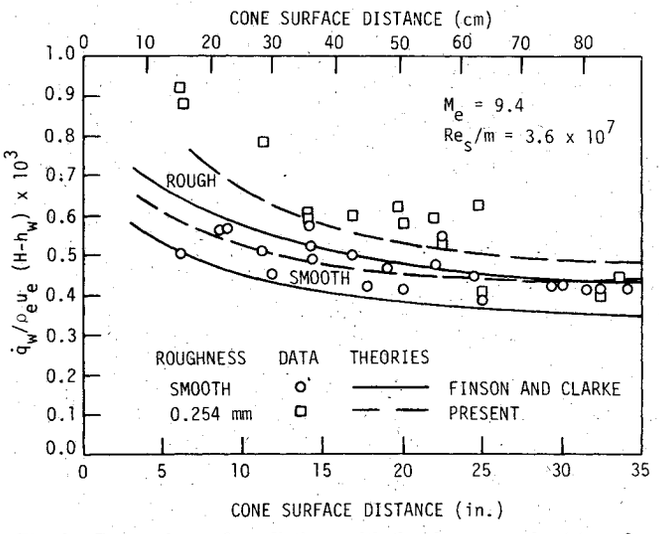

Fig. 9 Comparison of predictions with the sharp-cone heat-transfer data of Holden.

geometric progression such that the ratio of two adjacent normal coordinate increments was a constant. This ratio was set at 1.08 for the calculations reported here. Several features of the present difference procedure are as described by Harris.[18] For the final closure of Eqs. (8-10), the density is obtained from real-gas tables or from

$$\rho_w/\rho = T/T_w \tag{30}$$

for an ideal gas.

Skin friction coefficients are calculated from the smooth-wall contribution between roughness elements plus the form drag contribution

$$c_f = c_{f_s} + \frac{1}{2}\int_0^K \frac{u^2 c_D D(y) f(y)}{\rho_e u_e^2 L^2 B(y)}\,dy \tag{31}$$

Heat-transfer coefficients cannot be calculated in a similar manner because there is no heat-transfer mechanism analogous to form drag. A simple technique suggested by Finson and Clarke was adopted in this study. That is, the heat-transfer augmentation due to roughness is equal to the square root of the skin friction augmentation due to roughness. Physically, this is reasonable because velocity fluctuations are increased by roughness but temperature fluctuations are hardly changed by roughness and $\tau_w \sim \overline{u'v'}$ and $\dot{q}_w \sim \overline{v'T'}$.

Calculations

To test the validity of the difference formulation and the computer programming, a number of smooth-wall data comparisons were made. Two such comparisons, shown in Figs. 1 and 2, were made to AEDC smooth-wall, sphere/cone, and biconic heat-transfer data[19] taken at Mach 6. Figure 1 shows excellent agreement for the laminar heat-transfer predictions on a 7 deg sphere/cone. Predictions for the 14 deg/7 deg biconic turbulent heat transfer, shown in Fig. 2, are in good agreement with the data except in the turbulent region over the first cone. This overprediction could be a result of inaccurate transition region predictions that were performed using the intermittency formulation of Chen and Thyson.[20] For these blunt-body comparisons, the inviscid flow was calculated by the method described in Ref. 21, and the entropy-swallowing effects were treated by a mass balance and isentropic expansion as discussed in Ref. 22.

So far, several comparisons to rough-wall experimental data have been made. First, comparisons were made to Schlichting's incompressible flow data,[16] where various

arrangements of roughness elements, shown in Fig. 3, were used. Figure 4 gives skin friction coefficients vs distance Reynolds number (as presented by Finson and Clarke) for spherical segments with element spacings of $L/D(0)=2.5$ and 5. The present predictions are in excellent agreement with the data, correctly predicting the effect of spacing. The predictions of Finson and Clarke are also shown in Fig. 4. It should be mentioned that in the present calculations, the transformed coordinate η became very large, 100-200. A better turbulent grid generation scheme for these types of flows should be used, such as that proposed by Carter et al.[23]

The incompressible flow experiments of Healzer et al.[8] provided data on skin friction, heat transfer, and profiles for rough surfaces with and without blowing. The rough surface consisted of a regular array of tightly packed hemispherical $[L/D(0)=1]$ elements, each 0.127 cm in diameter. Tests were run at freestream velocities of 9.8, 42.4, and 73.8 m/s and blowing fractions ($\rho_w v_w/\rho_e u_e$) of 0.002 and 0.004. Skin friction and heat-transfer predictions are shown in Figs. 5 and 6 for $u_e=42.4$ m/s and $\rho_w v_w/\rho_e u_e=0.0$ and 0.004. Good agreement is shown for the no-blowing case, but calculations are about 25% high when blowing is present. The combined roughness/blowing effect in the proposed turbulence model needs improving. A plot of a calculated velocity profile vs the rough-wall data of Healzer et al. is shown in Fig. 7. The agreement looks good, although no data are given for small values of y^+.

For hypersonic flow over rough surfaces, comparisons were first made to the heat-transfer data of Hill et al.[24] taken on a 7 deg sharp cone at an edge Mach number of 8. The wall temperature ratio, T_w/T_{total}, was approximately 0.26. Following Finson and Clarke, the roughness elements were taken to be hemispheres spaced at 2.9 times the element heights. The predictions shown in Fig. 8 are in fair agreement with the data. In disagreement with the data, a strong distance dependence was found for the heat transfer by both the present method and that of Finson and Clarke. Finally, comparisons are shown for Holden's 6 deg sharp-cone data.[25] This experiment is similar to that of Hill et al. except that the edge Mach number is 9.4. Following Finson and Clarke, the sand grain roughness was simulated with tightly packed hemispheres $[L/D(0)=1.125]$. Roughness heights of 0.102 and 0.254 mm were tested. Figure 9 compares the present theory of Holden's data and to Finson and Clarke's calculations for a smooth surface and for a roughness of 0.254 mm. Although the present predictions are higher, both methods show about the same relative increase due to roughness. Neither method is able to predict the relative insensitivity of heat transfer to roughness as indicated by Holden's data for the aft end of the cone. Lin and Bywater's calculations,[10] on the other hand, show a decrease in heat transfer with increasing surface roughness along the entire cone (over a 25% decrease for the 0.254 mm roughness height).

Conclusions/Recommendations

A fully implicit finite difference solution to the boundary-layer equations for compressible flow with combined roughness and blowing is presented. To account for roughness effects, the boundary-layer equations are recast in the manner suggested by Finson and Clarke. A two-layer algebraic mixing length model that accounts for low Reynolds numbers, surface roughness, and mass addition is proposed. The difference equations are solved by the Thomas algorithm in an uncoupled manner in the order of streamwise momentum, continuity, and energy. Good agreement is shown for several comparisons to rough-wall, flat-plate, and sharp-cone data.

Several extensions/improvements to the method described in this paper are suggested:

1) The form drag coefficient and spacing between elements should be allowed to vary.

2) The effect of one element on another should be included.

3) History effects should be included in the turbulence model.

4) The combined roughness/blowing effect needs improving.

Even with all of the above capabilities, one of the most significant shortcomings of a roughness analysis remains. A procedure for characterizing a rough surface is needed.

Acknowledgments

This effort was supported by the General Electric Company, Re-entry Systems Division, Philadelphia, Pa. The interest and cooperation of V. Corbo, IR&D Program Manager, is gratefully acknowledged.

References

[1] Holden, M., "Studies of Aero-Thermodynamic Phenomena Influencing the Performance of Hypersonic Re-entry Vehicles," Calspan Corp., Buffalo, N. Y., Rept. SAMSO-TR-79-47, April 1979.

[2] Bettermann, D., "Contribution a l'Etude de la Connection Forces Turbulente le Long de Plaques Rugueuses," *International Journal of Heat and Mass Transfer*, Vol. 9, 1966, pp. 153-164.

[3] Dirling, R. B. Jr., "A Method for Computing Roughwall Heat Transfer Rates on Re-entry Nosetips," AIAA Paper 73-763, July 1973.

[4] White, C. O. and Grabow, R. M., "Nosetip Design Technology Program Final Report, Vol. I, Pattern Roughness Methodology," Rept. SAMSO-TR-75-70, March 1975.

[5] Cebeci, T. and Chang, K. C., "Calculation of Incompressible Rough-Wall Boundary-Layer Flows," *AIAA Journal*, Vol. 16, July 1978, pp. 730-735.

[6] Rotta, J. C., "Turbulent Boundary Layers in Incompressible Flow," *Progress in Aerospace Science*, Vol. 2, 1962, pp. 1-219.

[7] Hodge, B. K. and Adams, J. C., "The Calculation of Compressible Turbulent, and Relaminarization Boundary Layers Over Smooth and Rough Surfaces Using an Extended Mixing-Length Hypothesis," AEDC-TR-77-96, Feb. 1978.

[8] Healzer, J. M., Moffat, R. J., and Kays, W. M., "The Turbulent Boundary Layer on a Porous Rough Plate: Experimental Heat Transfer with Uniform Blowing," AIAA Paper 74-680 and ASME Paper 74-HT-14 presented at the AIAA/ASME 1974 Thermophysics and Heat Transfer Conference, Boston, Mass., July 1974.

[9] Finson, M. L. and Clarke, A. S., "The Effect of Surface Roughness Character on Turbulent Re-entry Heating," AIAA Paper 80-1459, 1980.

[10] Lin, T. C. and Bywater, R. J., "Turbulence Models for High-Speed, Rough-Wall Boundary Layers," *AIAA Journal*, Vol. 20, March 1982, pp. 325-333.

[11] Pletcher, R. H., "Prediction of Transpired Turbulent Boundary Layers," *Journal of Heat Transfer*, Vol. 96, Feb. 1974, pp. 89-94.

[12] White, F. M. and Christoph, G. H., "A Simple Theory for the Two-Dimensional Compressible Turbulent Boundary Layer," *Journal of Basic Engineering, Transactions of ASME*, Sept. 1972, pp. 636-642.

[13] van Driest, E. R., "On Turbulent Flow Near a Wall," *Journal of the Aeronautical Sciences*, Vol. 23, Nov. 1956, pp. 1007-1011.

[14] Simpson, R. L., "The Turbulent Boundary Layer on a Porous Plate: An Experimental Study of the Fluid Dynamics with Injection and Suction," Ph.D. Thesis, Stanford University, Stanford, Calif., 1968.

[15] Christoph, G. H., "Law-of-the-Wall Analysis for Turbulent Heating on Rough Surfaces," AIAA Paper 82-0197, Jan. 1982.

[16] Schlichting, H., "Experimental Investigation of the Problem of Surface Roughness," NACA TM823, 1937; also *Boundary Layer Theory*, McGraw-Hill Book Co., New York, 1968.

[17] Pletcher, R. H., "Prediction of Turbulent Boundary Layers at Low Reynolds Numbers," *AIAA Journal*, Vol. 14, May 1976, pp. 696-698.

[18] Harris, J. E., "Numerical Solution of the Equations for Compressible, Laminar, Transitional, and Turbulent Boundary Layers and Comparisons with Experimental Data," NASA TR R-368, 1971.

[19] Hube, F. K., "Heat-Transfer, Surface-Pressure, and Boundary-Layer Surveys on Conic and Biconic Bodies With Boundary-Layer Trips at Mach Number 6," AEDC-TSR-78-V24, Aug. 1978.

[20] Chen, K. K. and Thyson, N. A., "Extension of Emmons' Spot Theory to Flows on Blunt Bodies," *AIAA Journal*, Vol. 9, May 1971, pp. 821-825.

[21] Daywitt, J., Brant, D., and Bosworth, F., "Computational Technique for Three-Dimensional Inviscid Flow Fields About Re-entry Vehicles," Rept. SAMSO TR-79-5, April 1978.

[22] Hecht, A. M. and Nestler, D. E., "A Three-Dimensional Boundary-Layer Computer Program for Sphere-Cone-Type Re-entry Vehicles," *Engineering Analysis and Code Description*, Vol. 1, AFFDL-TR-78-67, June 1978.

[23] Carter, J. E., Edwards, D. E., and Werle, M. J., "A New Coordinate Transformation for Turbulent Boundary Layer Flows," NASA CP 2166, Oct. 1980.

[24] Hill, J. A. F., Voisinet, R. L. P., and Wagner, D. A., "Measurements of Surface Roughness Effects on the Heat Transfer to Slender Cones at Mach 10," AIAA Paper 80-0345, 1980.

[25] Holden, M. S., "Experimental Studies of Surface Roughness, Entropy Swallowing and Boundary Layer Transition Effects on Skin Friction and Heat Transfer Distribution in High Speed Flows," AIAA Paper 82-0034, Jan. 1982.